Design of Enzyme-pH Electrodes

A theoretical framework useful for predicting the steady state response of enzyme-pH electrodes is developed. The model takes into account that the catalytic activity of the enzymes as well as the degree of dissociation of the product acids and bases is strongly dependent upon the local pH, and that buffering salts present in solution facilitate the transport of H^+ ions. It is shown that the electrode should operate under substrate diffusion-limited conditions and the concentration of H^+ ions should not have steep variations within the enzymic membrane. This condition can be fulfilled by adjusting the buffer concentration in the bulk solution. In the latter conditions the electrode response does not depend on the actual kinetics of the enzymic reaction, and can be predicted by an algebraic equation. The predictions are in excellent agreement with the experiments on penicillinase-pH and urease-pH electrodes.

Sasidhar Varanasi and R. L. Stevens
Department of Chemical Engineering
University of Toledo
Toledo, OH 43606

E. Ruckenstein
Department of Chemical Engineering
State University of New York
at Buffalo
Amherst, NY 14260

Introduction

Enzyme electrodes are novel biochemical sensors for monitoring a variety of species that cannot readily be analyzed by direct analytical techniques. These electrodes are potentially of value in clinical, environmental, and industrial applications (Gough and Andrade, 1973; Wingard et al., 1981). The principle is that the species of interest undergoes an enzyme-catalyzed chemical reaction that either yields products or involves cosubstrates which can be analyzed electrochemically. In practice, enzyme electrodes are made by wrapping a membrane containing the immobilized enzyme on an electrode that is sensitive to one of the products or unconsumed cosubstrates. Since the product-specific electrode senses the concentration of the product at the membrane face opposite the face exposed to the bulk solution, the overall response behavior of the enzyme electrode is determined by the steady state concentration distribution of the product within the membrane. The latter is governed by the coupled transport and reaction phenomena taking place in the enzymic membrane.

The concept of an enzyme electrode was first proposed by Clark and Lyons (1962). Updike and Hicks (1967) developed the first electrode by polymerizing a gelatinous glucose oxidase-containing membrane over a polarographic oxygen electrode. They used this electrode for monitoring glucose. Subsequently, enzyme electrodes were developed for several other important biochemicals such as alcohol (Clark, 1972), urea (Guilbault and Hrabankoua, 1970a), amino acids (Guilbault and Hrabankoua, 1970b, 1971), amygdalin (Llendo and Rechnitz, 1971), lactates (Williams et al., 1970), tyrosine (Guilbault and Shu, 1972; Berjonneau et al., 1974), and phenylalanine (Berjonneau et al., 1974). The latest advances have been recently reviewed by Guilbault (1984) and by Scheller et al. (1985). In most of the previously mentioned electrodes, the enzymic reaction involved one of the following few products: NH_4^+, CN^-, CO_2, or O_2. For these products, specific electrodes that can measure their concentrations are readily available.

The successful design of an enzyme electrode involves finding a suitable product-specific electrode with well-defined performance characteristics, namely, stability, selectivity, sensitivity, and linearity. Often, product-specific electrodes do not exhibit the necessary selectivity and stability. Furthermore, most ion-specific electrodes exhibit Nernstian (linear) response only over a limited range of ion concentrations, and deviate substantially at both high and low concentrations. These limitations of product-specific electrodes can severely impair the performance of enzyme electrodes.

Conventional glass pH electrodes exhibit selectivity and stability characteristics that are undoubtedly far superior to any other known electrodes. They also display Nernstian response over a very wide range of H^+ concentrations (1 to 10^{-14} M). More importantly, a plethora of enzyme-catalyzed reactions involve H^+ ion formation or consumption. Thus the utilization of conventional pH electrodes as the sensing component seems to offer a versatile and accurate enzyme electrode for monitoring a variety of substrates that produce or consume acids. Indeed, Nilsson et al. (1973) developed enzyme-pH electrodes for sensing glucose, urea, and penicillin-G by entrapping the enzymes

Correspondence concerning this paper should be addressed to Sasidhar Varanasi.

glucose oxidase, urease, and penicillinase, respectively, either in polyacrylamide gels or in cellophane membranes. They observed a highly reproducible response behavior of their electrodes, even at very low values of the concentration of the monitored substances. More recently, pH-sensitive enzymic field effect transistors (ENFET) have successfully been fabricated by Caras et al. (1985b,c) and Flanagan and Carroll (1986) for monitoring glucose and benzyl-penicillin. The physicochemical phenomena involved in the functioning of these electrodes are much more complex than those of other product-specific enzyme electrodes for the following three reasons.

First, the catalytic activity of enzymes is sensitive to the pH of their environment. Typically, a plot of enzymic activity vs. pH displays bell-shaped behavior (Bailey and Ollis, 1977). Therefore, in reactions involving the production or consumption of H^+ ions the nonuniform pH distribution that arises in the membrane due to the diffusional resistance encountered by the H^+ ions leads to a spatial variation of enzymic activity inside the membrane. The spatial dependence of the enzyme's activity affects the production of the acid, which in turn modulates the pH distribution itself. This feedback process determines the final pH value at the membrane face in contact with the pH electrode.

Second, buffers (weak acids) added to the bulk solution bathing the membrane can facilitate proton transport out of (or into) the membrane (Engasser and Horvath, 1974; Deem et al., 1978; Ruckenstein and Varanasi, 1984). In other words, the conjugate base of the acid-base pair forming the buffer acts as a carrier that binds H^+ ions reversibly and augments their transport from (or into) the membrane by creating an alternate diffusion path. This flux enhancement of protons by buffers strongly affects the electrode response.

Third, in most cases the acids and/or bases produced during the enzymatic reactions are weak in nature. If the product is a strong acid, it will completely dissociate into an H^+ ion and a conjugate base instantaneously upon formation, and the two species will diffuse through the membrane independently. However, when the product is a weak acid, it only dissociates partially. Hence, the transport of H^+ ions and of the conjugate base is coupled by the equilibrium requirement, and the response of the enzyme electrode will be a function of the degree of dissociation of the product.

This paper develops a theoretical framework to predict the steady state response behavior of enzyme-pH electrodes, a framework that accounts for each of these effects. The model allows for the simultaneous formation of an acid and a base in the enzymic reaction. By proper manipulation of the governing species conservation equations, the effect of facilitation of proton transport by externally added buffer as well as by the product weak acid and/or base is lumped into an apparent diffusivity D_{app}, which replaces the diffusivity of the H^+ ion in the reaction-diffusion equation. The resulting nonlinear, second-order differential equation with concentration-dependent diffusivity was solved numerically together with the substrate conservation equation. When the enzymic reaction in the membrane is controlled by substrate diffusion, the H^+ ion concentration at the membrane-electrode interface can be related to the bulk substrate concentration by an algebraic equation that does not involve any of the kinetic parameters of the specific enzymic system. Finally, the predictions of the present theoretical model are tested against the experimental data of Nilsson et al. (1973) for urea and penicillin-G with urease-pH and penicillinase-pH electrodes.

We recently were made aware of the experimental and numerical study of pH-enzymic sensors by Caras et al. (1985a,b,c) for enzymic reactions involving the formation of a single acid. These authors' simulation involves direct numerical integration of the relevant equations. In contrast, the algebraic equation proposed here can explain their experimental data in a more simple and direct way (Varanasi et al. 1987).

The Model

A schematic representation of the enzyme-pH electrode is shown in Figure 1. The stirring rate is assumed to be high enough to maintain the concentrations at the membrane-solution interface equal to those in the bulk solution. The bulk solution contains, in addition to the substrate, small amounts of an externally added buffer (weak acid), WH. The concentrations of different reaction products in the bulk solution are assumed to be negligible, and the bulk pH is fixed at the value pH^b.

The following enzyme-catalyzed hydrolysis reaction is considered:

$$S + \gamma_R H_2O \rightarrow \gamma_A AH + \gamma_B BOH + \gamma_p P, \qquad (1)$$

where S denotes the substrate; AH, BOH, and P denote the acidic, basic, and other products of the hydrolysis reaction, respectively; and the γ's are the stoichiometric coefficients. The acidic and/or basic products formed undergo instantaneously the following protonation-deprotonation reactions:

$$AH \underset{k_{bA}}{\overset{k_{fA}}{\rightleftharpoons}} A^- + H^+ \quad K_A = \frac{k_{fA}}{k_{bA}} \qquad (2)$$

and

$$BOH + H^+ \underset{k_{bB}}{\overset{k_{fB}}{\rightleftharpoons}} B^+ + H_2O \quad K_B = \frac{k_{fB}}{k_{bB}} \qquad (3)$$

where k's are rate constants and K_A and K_B are equilibrium constants.

Facilitation of proton transport by added buffer, WH

To gain some understanding of the role of the added buffer, let us first consider that both the acid AH and the base BOH formed in the enzymic reaction are strong (i.e., in reactions 2 and 3, K_A and K_B have very large values). Therefore, ($|\gamma_A - \gamma_B|$) moles of H^+ ions are liberated (or consumed) for

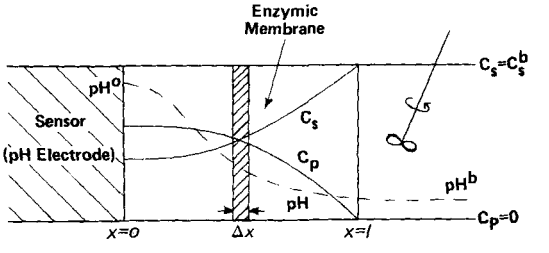

Figure 1. Enzyme electrode model.
Immobilized enzymic membrane extends from $x = 0$ to l.
Bulk solution in which enzyme electrode is dipped begins at $x = l$.

each mole of substrate consumed. The carrier mechanism of the added weak acid consists in the binding of these protons instantaneously to the conjugate base (i.e., W^-) according to the reversible reaction, Eq. 4, and the diffusion of the resulting WH species into the bulk solution if $(\gamma_A - \gamma_B) > 0$, and diffusion into the membrane if $(\gamma_A - \gamma_B) < 0$.

$$WH \underset{k_{bW}}{\overset{k_{fW}}{\rightleftharpoons}} W^- + H^+ \quad K_W = \frac{k_{fW}}{k_{bW}} \tag{4}$$

If the acidic and/or basic products of the enzymic reaction are weak (i.e., if K_A and K_B of reactions 2 and 3 are not large), the number of protons liberated (or consumed) per mole of substrate reacted will be smaller than $|\gamma_A - \gamma_B|$. The added buffer still enhances the transport of the liberated H^+ ions via the aforementioned mechanism. However, in this case the association-dissociation equilibria corresponding to reactions 2 and 3 must be satisfied at every location in the membrane.

Proton transport facilitation by weak acid and/or base products

A comparison of Eqs. 2 and 3 with Eq. 4 suggests that one can consider the products AH and/or BOH as additional proton transport facilitation agents present in the membrane together with the externally added weak acid. In other words, one can view the partial dissociation case as a complete dissociation case with the total amount of facilitation agent as the sum of the external buffer and the total acidic and/or basic product formed in reaction 1. One basic difference exists, however, between the facilitation caused by the product weak acids and/or bases and that resulting from the externally added buffer. In the latter case, the extent of facilitation can be controlled by fixing the total buffer concentration in the bulk solution, while in the former case, the rate of enzymic reaction itself determines the amount of products and hence the extent of facilitation. As shown later, the above viewpoint proves to be extremely useful in predicting and understanding the electrode response.

Governing equations

A steady state mass balance on a slice of differential thickness Δx in the enzymic membrane, Figure 1, leads, in the absence of convection, to the following differential equations for the various species:

Substrate

$$D_S \frac{d^2C_S}{dx^2} = R(C_{H^+}, C_S) \tag{5}$$

Product weak acid, AH

$$D_{AH} \frac{d^2C_{AH}}{dx^2} = -\gamma_A R(C_{H^+}, C_S) + r_A \tag{6}$$

Product weak base, BOH

$$D_{BOH} \frac{d^2C_{BOH}}{dx^2} = -\gamma_B R(C_{H^+}, C_S) + r_B \tag{7}$$

H^+ ion

$$D_{H^+} \frac{d^2C_{H^+}}{dx^2} = -r_A + r_B - r_W \tag{8}$$

A^- ion

$$D_{A^-} \frac{d^2C_{A^-}}{dx^2} = -r_A \tag{9}$$

B^- ion

$$D_{B^-} \frac{d^2C_{B^-}}{dx^2} = -r_B \tag{10}$$

W^- ion

$$D_{W^-} \frac{d^2C_{W^-}}{dx^2} = -r_W \tag{11}$$

Conjugate acid, WH

$$D_{WH} \frac{d^2C_{WH}}{dx^2} = r_W \tag{12}$$

where,

$$r_A = k_{fA}C_{AH} - k_{bA}C_{A^-}C_{H^+}, \tag{13}$$

$$r_B = k_{fB}C_{BOH}C_{H^+} - k_{bB}C_{B^-}, \tag{14}$$

and

$$r_W = k_{fW}C_{WH} - k_{bW}C_{W^-}C_{H^+}. \tag{15}$$

In the above equations, the D's are the diffusivities of the various species and the C's their concentration at any location within the membrane, r_i's ($i = A$, B, or W) denote the molar rates per unit volume of reactions 2, 3, and 4, respectively, and $R(C_{H^+}, C_S)$ represents the rate of the enzymic reaction (i.e., moles of substrate consumed per unit volume and unit time).

The pore structure of the membranes does not usually lead to any selective partitioning of the solutes into the membrane phase, and hence one can write the following boundary conditions at the membrane-solution interface:

$$C_S(x = \ell) = C_S^b \tag{16}$$

$$C_{AH} = C_{BOH} = C_{A^-} = C_{B^-} = 0 \quad \text{at } x = \ell \tag{17}$$

$$C_{H^+}(x = \ell) = C_{H^+}^b \tag{18}$$

$$C_{W^-}(x = \ell) + C_{WH}(x = \ell) = C_{TW}^b \tag{19}$$

where C_S^b and $C_{H^+}^b$ are the bulk concentrations of the substrate and protons, respectively, and C_{TW}^b is the total bulk concentration of the externally added buffer. Since the membrane-pH electrode interface is impenetrable to all species, the flux of each

is zero there:

$$\frac{dC_i}{dx}(x = o) = 0$$

$$\text{for } i = S, AH, BOH, H^+, A^-, B^-, W^-, \text{ and } WH \quad (20)$$

It should be noted that in Eqs. 5–12 one assumes that diffusion can be described by Fick's equation. In reality, charged species are involved in the transport process. During the diffusion of such ionic species, an electrical potential gradient (diffusion potential) develops in the medium in order to arrest the flow of electric current arising due to the different diffusivities and charges of the ions (Zabusky and Deem, 1979; Ruckenstein and Kalthod, 1982). The net effect of this electric field is to enhance the transport of the slower ions and retard the faster ions. Thus, transport of ions is coupled by the diffusion potential. However, the electric field and its effect on ion fluxes become negligible if the ionic strength of the medium is large enough. In most experimental systems the ionic strength is deliberately maintained high (>0.1 M) by adding a strong electrolyte to the system in order to suppress these electrical effects (Nilsson et al., 1973). Furthermore, in systems of high ionic strength in which the transport of various ionic species is facilitated by rapid chemical reactions, flux alterations caused by diffusion potential and differences in diffusion coefficients are much less significant compared to the flux changes resulting due to reaction-diffusion coupling (Ruckenstein and Varanasi, 1982). Therefore, it will be assumed that Fick's law is valid and the individual diffusion coefficients of the ions will be replaced by an effective diffusion coefficient D, which is assumed to be the same for all ions. Further, for the sake of simplicity, it will be assumed that the diffusion coefficient of the uncharged species is also equal to D.

Simplification of the equations

The continuity equations, Eqs. 5–12, are rewritten in such a manner that they do not explicitly involve the intrinsic reaction rates of the instantaneous reactions 2, 3, and 4. This is achieved by defining "composite species":

$$C_{TA} = C_{AH} + C_{A^-} \quad (21)$$

$$C_{TB} = C_{BOH} + C_{B^-} \quad (22)$$

and

$$C_{TW} = C_{WH} + C_{W^-} \quad (23)$$

where C_{TA}, C_{TB}, and C_{TW} are the total, that is the sums of dissociated and undissociated, concentrations of the species AH, BOH, and WH at any location within the membrane. Using Eqs. 21–23, Eqs. 5–12 become:

$$D\frac{d^2C_S}{dx^2} = R(C_{H^+}, C_S) \quad (24)$$

$$D\frac{d^2C_{TA}}{dx^2} = -\gamma_A R(C_{H^+}, C_S) \quad (25)$$

$$D\frac{d^2C_{TB}}{dx^2} = -\gamma_B R(C_{H^+}, C_S) \quad (26)$$

$$D\frac{d^2C_{TW}}{dx^2} = 0 \quad (27)$$

$$D\frac{d^2C_{H^+}}{dx^2} + D\frac{d^2C_{AH}}{dx^2} - D\frac{d^2C_{BOH}}{dx^2} + D\frac{d^2C_{WH}}{dx^2} = -(\gamma_A - \gamma_B)R(C_{H^+}, C_S) \quad (28)$$

$$D\frac{d^2C_{A^-}}{dx^2} = -k_{bA}(K_AC_{AH} - C_{A^-}C_{H^+}) \quad (29)$$

$$D\frac{d^2C_{B^-}}{dx^2} = -k_{bB}(K_BC_{BOH}C_{H^+} - C_{B^-}) \quad (30)$$

$$D\frac{d^2C_{W^-}}{dx^2} = -k_{bW}(K_WC_{WH} - C_{W^-}C_{H^+}) \quad (31)$$

Since the protonation-deprotonation rates involving conjugate acid-base pairs are extremely fast, in each of the Eqs. 29–31 the characteristic time of either the forward or the backward reactions is much smaller than the characteristic time for diffusion of the species through the membrane. Consequently, it is legitimate to replace Eqs. 29–31 with the following three approximations:

$$K_AC_{AH} - C_{A^-}C_{H^+} \simeq 0 \quad (32)$$

$$K_BC_{BOH}C_{H^+} - C_{B^-} \simeq 0 \quad (33)$$

$$K_WC_{WH} - C_{W^-}C_{H^+} \simeq 0 \quad (34)$$

This leads to:

$$C_{AH} = \frac{C_{TA}C_{H^+}}{K_A + C_{H^+}} \quad (35)$$

$$C_{BOH} = \frac{C_{TB}}{1 + K_BC_{H^+}} \quad (36)$$

and

$$C_{WH} = \frac{C_{TW}C_{H^+}}{K_W + C_{H^+}} \quad (37)$$

Substitution of Eqs. 35–37 into Eq. 28 leads to:

$$D\frac{d}{dx}\left[\frac{dC_{H^+}}{dx} + \frac{d}{dx}\left(\frac{C_{TA}C_{H^+}}{K_A + C_{H^+}}\right) - \frac{d}{dx}\left(\frac{C_{TB}}{1 + K_BC_{H^+}}\right) + \frac{d}{dx}\left(\frac{C_{TW}C_{H^+}}{K_W + C_{H^+}}\right)\right] = -(\gamma_A - \gamma_B)R(C_{H^+}, C_S) \quad (38)$$

The subsequent analysis is based on the system of Eqs. 24–27 and 38, whose dimensionality is smaller than that of the original system by three units.

Apparent diffusivity of protons in the presence of weak acids and/or bases and buffer

Integrating Eq. 27 subject to the boundary conditions: (1) that the flux of the species is zero at the membrane-electrode interface, and (2) that the total added buffer concentration in the stirred solution, C^b_{TW}, is known, one obtains

$$C_{TW}(x) = C^b_{TW} = \text{constant} \tag{39}$$

Therefore, Eq. 38 becomes:

$$\frac{d}{dx}\left(D_{app}\frac{dC_{H^+}}{dx}\right) = -(\gamma_A - \gamma_B)R(C_{H^+}, C_S), \tag{40}$$

where

$$D_{app} = D\left[1 + \frac{C^b_{TW}K_W}{(K_W + C_{H^+})^2} + \frac{C_{TA}K_A}{(K_A + C_{H^+})^2} + \frac{C_{TB}K_B}{(1 + K_BC_{H^+})^2} + \left(\frac{C_{H^+}}{K_A + C_{H^+}}\right)\left(\frac{dC_{TA}}{dC_{H^+}}\right) - \frac{1}{(1 + K_BC_{H^+})}\left(\frac{dC_{TB}}{dC_{H^+}}\right)\right] \tag{41}$$

An examination of the second, third, and fourth terms of the latter expression indicates that the product acid and/or base, when weak, augments the transport of H^+ ions through the membrane in a way very similar to that of the externally added buffer. It is possible to derive explicit expressions relating C_{TA} and C_{TB} to C_{H^+}. These relations will enable one to express the apparent diffusivity of protons as a function of C_{H^+} only, and thus to reduce Eq. 40 to a reaction-diffusion equation for protons with a concentration dependent diffusion coefficient.

Functional dependence of C_{TA} and C_{TB} on C_{H^+}

First, $R(C_{H^+}, C_S)$ can be eliminated between Eqs. 25 and 26 to obtain

$$\frac{1}{\gamma_A}\frac{d^2C_{TA}}{dx^2} = \frac{1}{\gamma_B}\frac{d^2C_{TB}}{dx^2} \tag{42}$$

Integrating Eq. 42 twice with respect to x, subject to the boundary conditions that (1) the fluxes of both TA and TB vanish at $x = 0$, and (2) TA and TB have negligible concentration levels in the bulk solution, leads to

$$C_{TA}(x) = \frac{\gamma_A}{\gamma_B}C_{TB}(x) \tag{43}$$

Similarly, one can also eliminate $R(C_{H^+}, C_S)$ between Eqs. 38 and 25, and the resulting equation can be integrated once with respect to x to obtain

$$D\frac{dC_{H^+}}{dx} + D\frac{d}{dx}\left(\frac{C_{TA}C_{H^+}}{K_A + C_{H^+}}\right) - D\frac{d}{dx}\left(\frac{C_{TB}}{1 + K_BC_{H^+}}\right) + D\frac{d}{dx}\left(\frac{C_{TW}C_{H^+}}{K_W + C_{H^+}}\right) = D\frac{(\gamma_A - \gamma_B)}{\gamma_A}\frac{dC_{TA}}{dx} + Q \tag{44}$$

The integration constant, Q, is zero because the quantities in the brackets on the lefthand side of Eq. 44 are C_{AH}, C_{BOH}, and C_{WH}, respectively—see Eqs. 35–37—and the fluxes of all species vanish at $x = 0$. Upon substituting Eqs. 39 and 43, Eq. 44 reduces to:

$$\frac{dC_{TA}}{dC_{H^+}} = \left[\frac{K_A}{(K_A + C_{H^+})^2} + \frac{(\gamma_B/\gamma_A)K_B}{(1 + K_BC_{H^+})^2}\right]C_{TA} + \frac{\left[1 + \frac{C^b_{TW}}{(K_W + C_{H^+})^2}\right]}{\left[\frac{K_A}{(K_A + C_{H^+})} + \frac{(\gamma_B/\gamma_A)K_BC_{H^+}}{(1 + K_BC_{H^+})}\right]} \tag{45}$$

Solving Eq. 45 for the boundary condition that C_{TA} is negligible in the bulk yields:

$$C_{TA} = \frac{(C_{H^+} - C^b_{H^+})\left[1 + \frac{C^b_{TW}K_W}{(K_W + C^b_{H^+})(K_W + C_{H^+})}\right]}{\left[\frac{K_A}{(K_A + C_{H^+})} - \frac{(\gamma_B/\gamma_A)K_BC_{H^+}}{(1 + K_BC_{H^+})}\right]} \tag{46}$$

One can now express easily C_{TA}, C_{TB}, dC_{TA}/dC_{H^+}, and dC_{TB}/dC_{H^+} in Eq. 41 in terms of C_{H^+}, with the help of Eqs. 43, 45, and 46 to obtain:

$$\frac{D_{app}}{D} = \frac{(\gamma_A - \gamma_B)\left[1 + \frac{C^b_{TW}K_W}{(K_W + C_{H^+})^2}\right]}{\left[\frac{\gamma_AK_A}{(K_A + C_{H^+})} - \frac{\gamma_BK_BC_{H^+}}{(1 + K_BC_{H^+})}\right]} + \frac{(\gamma_A - \gamma_B)(C_{H^+} - C^b_{H^+})\left[1 + \frac{C^b_{TW}K_W}{(K_W + C^b_{H^+})(K_W + C_{H^+})}\right]\left[\frac{\gamma_AK_A}{(K_A + C_{H^+})^2} + \frac{\gamma_BK_B}{(1 + K_BC_{H^+})^2}\right]}{\left[\frac{\gamma_AK_A}{(K_A + C_{H^+})} - \frac{\gamma_BK_BC_{H^+}}{(1 + K_BC_{H^+})}\right]^2} \tag{47}$$

Equation 47 relates the apparent diffusivity of protons to the local H^+ ion concentration, the pK and the total concentration of the added buffer in the bulk solution, the stoichiometric coefficients and the protonation-deprotonation equilibrium constants of the acid and/or base products, and the pH of the bulk solution. Substituting this expression for D_{app} into the overall reaction-diffusion equation for protons, Eq. 40, decouples the latter from all the dependent variables except the substrate concentration, which appears in the rate expression $R(C_{H^+}, C_S)$. Therefore, Equations 40 and 24 have to be solved simultaneously to determine the electrode response.

Substrate concentration expressed in terms of proton concentration

The addition of Eqs. 24 and 40 leads to

$$D\frac{d^2C_S}{dx^2} + \frac{1}{\gamma_A - \gamma_B}\frac{d}{dx}\left(D_{app}\frac{dC_{H^+}}{dx}\right) = 0 \qquad (48)$$

Integrating and using the boundary conditions given in Eq. 20, one obtains

$$D\frac{dC_S}{dx} + \frac{D_{app}}{\gamma_A - \gamma_B}\frac{dC_{H^+}}{dx} = 0 \qquad (49)$$

Using Eq. 47 for D_{app}, Eq. 49 can be integrated once more across the membrane thickness for the boundary conditions of Eq. 16 and 18, to obtain:

$$C_S^b = C_S^o + (C_{H^+}^o - C_{H^+}^b)\left[1 + \frac{C_{TW}^b K_W}{(K_W + C_{H^+}^b)(K_W + C_{H^+}^o)}\right] \cdot \left[\frac{1}{\dfrac{(\gamma_A K_A)}{(K_A + C_{H^+}^o)} - \dfrac{(\gamma_B K_B C_{H^+}^o)}{(1 + K_B C_{H^+}^o)}}\right] \qquad (50)$$

Equation 50 can be used to determine the electrode response for any C_S^b provided that the corresponding value of C_S^o is known. When the enzymic reaction is substrate diffusion-limited, C_S^o becomes negligibly small compared to C_S^b, and Eq. 50 allows one to predict the electrode response without knowing the actual kinetics of the enzymic reaction and the diffusion coefficients.

Model Predictions and Comparison with Experimental Data

Due to its mathematical complexity, the above general formulation does not provide enough insight into the various phenomena associated with the electrode performance when C_S^o is not small. In order to remedy this situation, one can consider, successively, the following three types of electrodes in which the enzymic reaction produces:

1. Only an acid or a base that is strong
2. Only an acid or a base that is weak
3. Both an acid and a base that are weak

Most experimentally studied enzyme-pH electrode systems fall into one of the above three categories. The hydrolysis of glucose in the presence of oxygen to gluconic acid by glucose oxidase

$$\text{glucose} + O_2 + H_2O \rightarrow \text{gluconic acid} + H_2O_2 \qquad (51a)$$

constitutes an example for case 1, because gluconic acid ($pK_A \sim 3.5$) undergoes essentially complete dissociation for $pH > 4$.

$$\text{penicillin-G} + H_2O \rightarrow \text{penicilloic acid} \qquad (51b)$$

involving the hydrolysis of the β-lactam ring of penicillin-G by the enzyme penicillinase (β-lactamase) serves as an example for case 2, since penicilloic acid ($pK_A \sim 6.4$) dissociates only partially in the pH range of 5–8. Finally, the hydrolysis of urea by the enzyme urease

$$H_2NCONH_2 + 2H_2O \rightarrow H_2CO_3 + 2NH_3 \qquad (51c)$$

constitutes an example of case 3 since it involves the production of both an acid (H_2CO_3) and a base (NH_3), both of which undergo partial protonation-deprotonation over a wide range of pH.

$$H_2CO_3 \rightleftharpoons HCO_3^- + H^+ \qquad (51d)$$

$$NH_3 + H^+ \rightleftharpoons NH_4^+ \qquad (51e)$$

Reaction mechanism

The rate R is given by the Michaelis-Menten kinetics:

$$R = \frac{V_{max}C_S}{K_M + C_S}, \qquad (52)$$

where V_{max} is the maximum limiting rate obtained for a very large substrate concentrations C_S, and K_M is the Michaelis constant. The values of the parameters V_{max} and K_M depend upon the pH of the medium.

For a variety of enzymes, the monoionized form of a diacidic side group of the enzyme constitutes the catalytically active site, and either protonation or deprotonation of this monoionized state renders the group inactive (Cornish-Bowden, 1979). For such enzymes, V_{max} is given by (Cornish-Bowden, 1979):

$$V_{max} = \frac{ke_o}{\left(1 + \dfrac{C_{H^+}}{K_1} + \dfrac{K_2}{C_{H^+}}\right)} \qquad (53)$$

where k is the rate constant for the irreversible decomposition of the monoionized enzyme-substrate complex into products, e_o is the total enzyme concentration, and K_1 and K_2 are the equilibrium constants for the protonation and deprotonation reactions that deactivate the monoionized state. Furthermore, K_M for such enzymes can be considered to be independent of pH. Therefore, one obtains for R:

$$R(C_{H^+}, C_S) = \left[\frac{V^*}{\left(1 + \dfrac{C_{H^+}}{K_1} + \dfrac{K_2}{C_{H^+}}\right)}\right]\left(\frac{C_S}{K_M + C_S}\right) \qquad (54)$$

where $V^* = ke_o$.

Equation 54 will be employed for most of the following analysis. However, while comparing the model predictions with the experimental data of a given enzymic system, the actual expressions describing the pH dependence of V_{max} and K_M for that system will be used if they are different from Eq. 54. (Equations 40 and 24 were solved simultaneously using the technique of orthogonal collocation on finite elements [Carey and Finlayson, 1975] after substituting Eq. 54 for R.)

Case 1. Enzymic reaction produces a strong acid with $\gamma_A = 1$

No Added Buffer Present. In this case $C_{TW}^b = 0$ and the pair of differential equations governing the electrode response are:

$$D\frac{d^2C_S}{dx^2} = \frac{V^*}{\left(1 + \dfrac{C_{H^+}}{K_1} + \dfrac{K_2}{C_{H^+}}\right)}\frac{C_S}{(K_M + C_S)} \qquad (55)$$

and

$$D\frac{d^2C_{H^+}}{dx^2} = \frac{-V^*}{\left(1 + \frac{C_{H^+}}{K_1} + \frac{K_2}{C_{H^+}}\right)}\left(\frac{C_S}{K_M + C_S}\right) \tag{56}$$

To determine the electrode response, Eqs. 55 and 56 must be solved for the boundary conditions of Eqs. 16, 18, and 20. It is convenient to cast Eqs. 55–56 into the following dimensionless form:

$$\frac{d^2\bar{C}_S}{d\xi^2} = \phi^2\left(\frac{\bar{C}}{\bar{C}^2 + \bar{C} + \chi}\right)\frac{\bar{C}_S}{1 + \bar{C}_S} \tag{57}$$

and

$$\frac{d^2\bar{C}}{d\xi^2} = -\phi^2\lambda\left(\frac{\bar{C}}{\bar{C}^2 + \bar{C} + \chi}\right)\frac{\bar{C}_S}{1 + \bar{C}_S}, \tag{58}$$

where $\xi = (x/\ell)$, $\bar{C} = (C_{H^+}/K_1)$, $\bar{C}_S = (C_S/K_M)$, $\chi = (K_2/K_1)$, $\lambda = (K_M/K_1)$, and $\phi = (V^*\,\ell^2/DK_M)^{1/2}$. The parameter ϕ is the Thiele modulus, which represents the ratio of the characteristic time of diffusion of the substrate to that of its reaction within the membrane.

It has been recognized (Blaedel et al., 1972, Brady and Carr, 1980; Gough and Leypoldt, 1981) that ϕ is a valuable parameter in the design of enzyme electrodes. To demonstrate its role, and to streamline the ensuing discussion, it is instructive to recapitulate the important conclusions of Brady and Carr's simulation of a product-sensitive enzyme electrode which does not involve generation or consumption of acids. In this case, Eq. 57 assumes a much simpler form because the term in the parenthesis is a constant. (This constant will have its optimal value F^o if the bulk solution is at the enzyme's optimal pH). Equation 57 can then be solved separately to determine the substrate concentration at $x = 0$ (C_S^o) which, in turn, can be used to determine the concentration of the product of interest at the sensor surface, C_p^o, using the following relation:

$$C_p^o = C_S^b - C_S^o \tag{59}$$

which is obtained by adding the conservation equations for the substrate and the product of interest and integrating the resulting equation with the appropriate boundary conditions across the membrane thickness.

Solution of Eq. 57 reveals that when $\phi'(=\phi\sqrt{F^o})$ is large, C_S^o is negligible compared to C_S^b up to C_S^b values $\gg K_M$; thus the response of the electrode is linear to high bulk substrate concentrations; see Eq. 59. However, for low values of ϕ', the signal for a given bulk substrate concentration is significantly reduced and becomes nonlinear because C_S^o is not negligible compared to C_S^b. The substrate concentration up to which linearity is desired dictates the minimal required value of ϕ'. Brady and Carr established that the response of the electrode for a specific bulk substrate concentration is linear provided that the value of ϕ' for the electrode satisfies the following inequality:

$$\phi' \geq 2.08\left(\frac{C_S^b}{K_M}\right)^{0.4} \tag{60}$$

Returning to the enzyme-pH electrodes, the above conclusions on product-sensitive electrodes suggest that designing these electrodes with a high value of ϕ may ensure linear response of the electrode over a wide range of substrate concentrations. However, the case of enzyme-pH electrodes is more complicated. The activity of enzymes as a function of pH passes through an optimum, as depicted in Figure 2. Thus, even when the bulk solution bathing the membrane is maintained at the optimal pH of the enzyme, the diffusional resistance encountered, at the proposed high values of ϕ, by the H^+ ions produced in the enzymic reaction leads to a significant pH depression within the membrane. This causes a drastic reduction in the catalytic activity of the enzymic membrane in accordance with the activity behavior displayed in Figure 2. In other words, the effective value of $\phi'(=\phi\sqrt{F})$ for enzyme-pH electrodes will become much lower than $\phi\sqrt{F^o}$ and thus the electrode exhibits saturation characteristics at much lower values of C_S^b compared to a product-sensitive electrode operating under identical conditions.

In Figure 3a the H^+ ion and substrate concentration distributions (obtained by solving Eqs. 57 and 58) are plotted at different C_S^b values for an enzymic reaction with a pH activity behavior corresponding to that of Figure 2, and having a K_M of 7.7×10^{-5} M; the ϕ value is 18.8 and pH^b is 6.75. Even at this moderate value of ϕ, the pH within the membrane falls by several units with respect to its bulk value, starting from very low values of C_S^b (i.e., $C_S^b \leq K_M$). In fact, for bulk substrate concen-

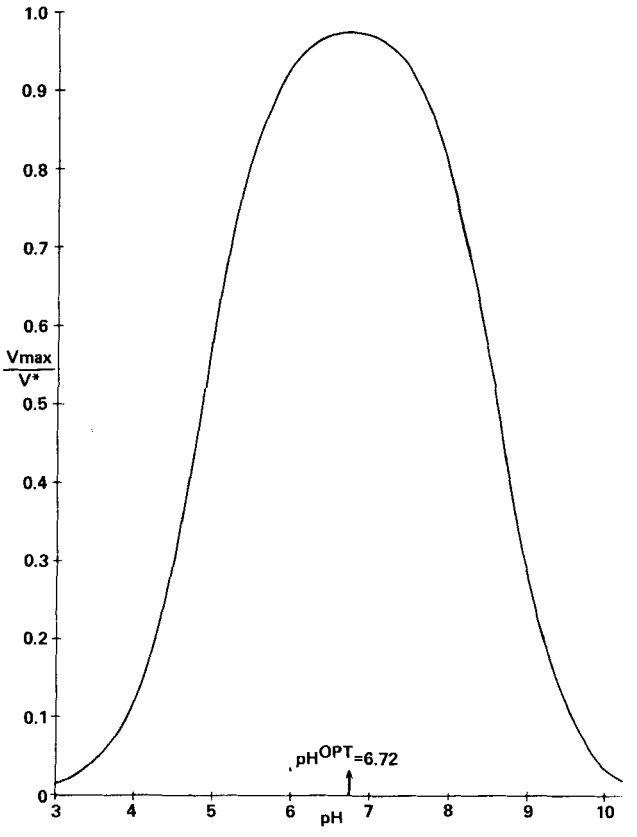

Figure 2. Normalized activity V_{max}/V^* of enzyme penicillinase (β-lactamase) as a function of pH.
$K_1 = 10^{-4.85}$ M, $K_2 = 10^{-8.6}$ M; see Eq. 53.

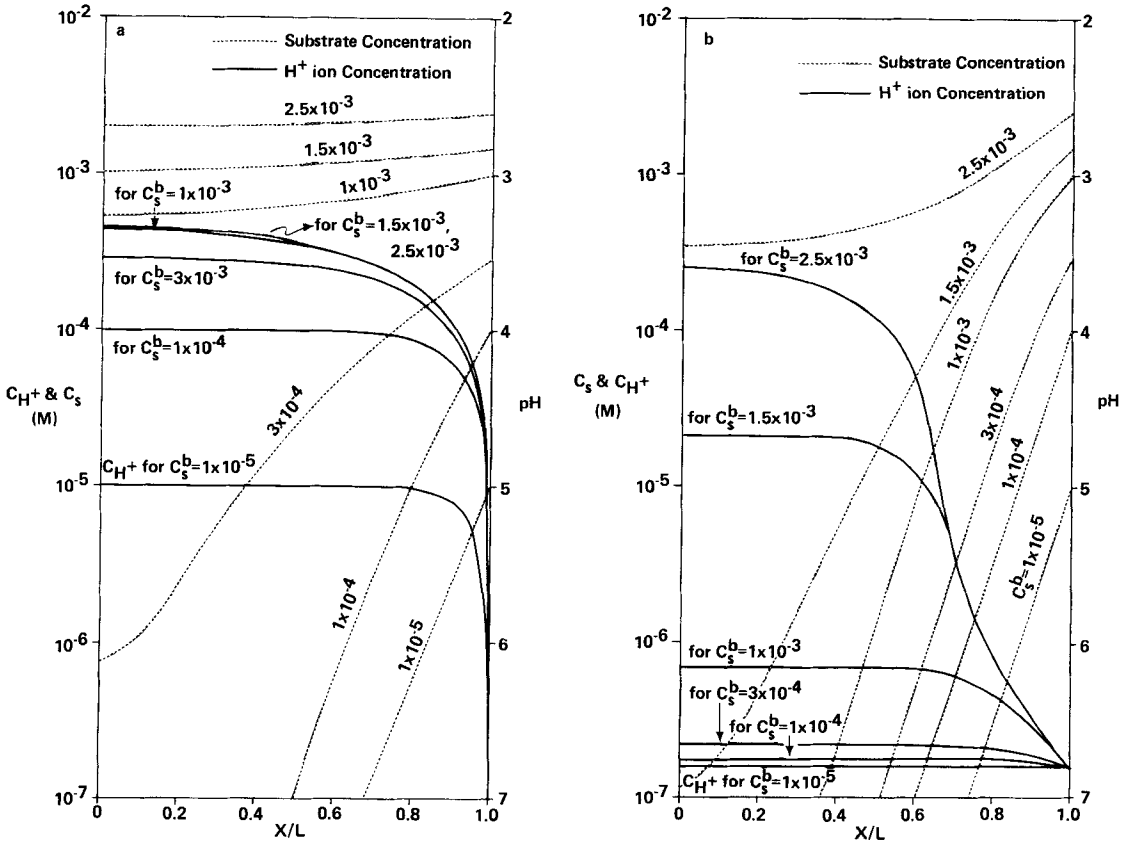

Figure 3. Computed intramembrane substrate and pH distribution profiles for a hypothetical enzyme with the same K_1, K_2 values as penicillinase, but producing a stronger acid.
Figure 3a. No external buffer present in bulk solution.
Figure 3b. Buffer of pK 7.21 added to bulk solution at concentration level of 5×10^{-3} M.

trations as small as 2.5×10^{-4} M (which is only about 3.5 times the K_M), the internal pH in most of the membrane has already fallen to a value of less than 4, which reduces the activity to about 10% of its value at the bulk pH; see Figure 2. It can also be noted from the figure that the fractional change in substrate concentration between the two faces of the membrane, $f = [(C_S^b - C_S^o)C_S^b]$, decreases as C_S is raised, changing from a value of unity at low C_S^b values to about 0.45 for $C_S^b \sim 1.0 \times 10^{-3}$ M. As can be seen from Eq. 59, this decrease in fractional drop of substrate concentration across the membrane leads first to nonlinearity in the electrode response, followed by eventual saturation. Curve *a* of Figure 4, which depicts the computed response behavior of the electrode, indicates that the electrode does indeed saturate for $C_S^b \geq 6\ K_M$, and the response becomes nonlinear for values of C_S^b around 3 K_M. However, Eq. 60 of Brady and Carr indicates that for product sensitive electrodes, linear response is obtained at this value of ϕ to at least 6 K_M. Therefore, this premature saturation of the electrode is a manifestation of the loss in activity of the membrane due to the pH depression.

Since the response characteristics of the enzyme-pH electrodes are impaired by the diffusional limitations on the H^+ ions, one can expect the externally added weak acids, which facilitate the transport of these ions, to be able to modify the response behavior significantly.

Effect of Buffers on Strong-Acid Electrodes. To compute the response behavior in the presence of an external buffer, one has to solve Eq. 55 together with the equation:

$$\frac{d}{dx}\left(D_{app}\frac{dC_{H^+}}{dx}\right) = \frac{-V^*}{\left(1 + \dfrac{C_{H^+}}{K_1} + \dfrac{K_2}{C_{H^+}}\right)}\frac{C_S}{(K_M + C_S)} \tag{61}$$

where

$$D_{app} = D\left[1 + \frac{(C_{TW}^b/K_W)}{\left(1 + \dfrac{C_{H^+}}{K_W}\right)^2}\right] \tag{62}$$

Equation 62 for D_{app} is obtained by setting $\gamma_A = 1$, $\gamma_B = 0$, and $K_A \rightarrow \infty$ in Eq. 47. It shows that at a given value of the total concentration of the added acid, C_{TW}^b, the ratio (D_{app}/D):

1. Is close to unity for pH values much below pK_w
2. Can become orders of magnitude larger than unity for pH values higher than pK_w
3. Can be maximized, for any given pH, by choosing a buffer whose pK is equal to the pH.

In view of this interesting dependence of D_{app} on its parameters, maximum advantage, in terms of alleviating the adverse pH gradients in the membrane, can be gained by using a buffer

with a pK equal or close to the bulk pH, at a concentration level dictated by the Thiele modulus of the electrode. Of course, the natural choice for the pH of the bulk solution is the pH corresponding to the optimal activity of the native enzyme.

Figure 3b clearly shows that an added weak acid, satisfying the above criteria, can create, even when present at very small concentrations, a dramatic alteration in the intramembrane pH distribution. Indeed, for bulk substrate concentrations comparable to or smaller than K_M, the pH gradients in the membrane have essentially been eliminated, making $C^o_{H^+}$ almost equal to $C^b_{H^+}$. At higher values of C^b_S, however, the proton transport facilitation by the added acid does not lead to a total elimination of the pH gradient, although the difference in the pH values at the two faces of the membrane, $\Delta pH (= pH^o - pH^b)$, has been considerably reduced. It is pertinent to note that buffers are added to the bulk solution in order to alleviate drastic pH gradients in the membrane that severely limit the range of C^b_S values over which the electrode response is linear. One must not, however, totally eliminate the pH gradients, because the very principle on which the enzyme-pH electrodes function is to monitor the variation of pH^o relative to pH^b for a specified change in C^b_S. Thus, the larger the change in pH^o for a specified change in C^b_S, the higher is the intensity of response of the electrode. On one hand, large changes in the membrane pH are desirable because they lead to strong electrode signals. On the other hand, too large changes are deleterious to the electrode performance because they tend to deactivate the enzyme. The strategy, therefore, is to use an appropriate amount of external buffer, which will reduce the pH gradients to an extent sufficient to maintain the membrane at a fairly high activity level over a large range of C^b_S values, while permitting a perceptible and measurable variation in pH^o with changing values of C^b_S. A comparative examination of the response of the electrode, in the presence and absence of the external buffer, displayed in Figure 4, shows that a concentration level of 5×10^{-3} M of the added weak acid does indeed achieve the desired effect. In the range of C^b_S values for which, in the absence of added weak acid, the electrode exhibits saturation characteristics, measurable responses become possible in the presence of added buffer.

Finally, one may note that, unlike Figure 3a, in Figure 3b the transmembrane fractional substrate concentration drop, f, is very close to unity over the entire range of C^b_S values considered. One may also recall that when $f \rightarrow 1$, (i.e., when $C^o_S \ll C^b_S$), a linear response behavior is expected from the electrode in the absence of buffer. However, when $f \rightarrow 1$ one obtains the following simple algebraic equation relating pH^o to C^b_S in the presence of an added buffer, when the product acid is strong:

$$C^b_S = (C^o_{H^+} - C^b_{H^+})\left[1 + \frac{C^b_{TW} K_W}{(K_W + C^b_{H^+})(K_W + C^o_{H^+})}\right] \quad (63)$$

This equation is obtained from Eq. 50 by setting $\gamma_B = 0$, letting $K_A \rightarrow \infty$, and considering $C^b_S \gg C^o_S$. Over the entire range of C^b_S values for which C^b_{TW} can bring the value of f close to unity, Eq. 63 can predict the electrode response.

All of the above conclusions drawn for strong acids are equally valid when the enzymic reaction produces instead a strong base, the only difference being that in the latter case, $pH^o > pH^b$, while in the former $pH^o < pH^b$. The corresponding equations describing the electrode performance for the strong

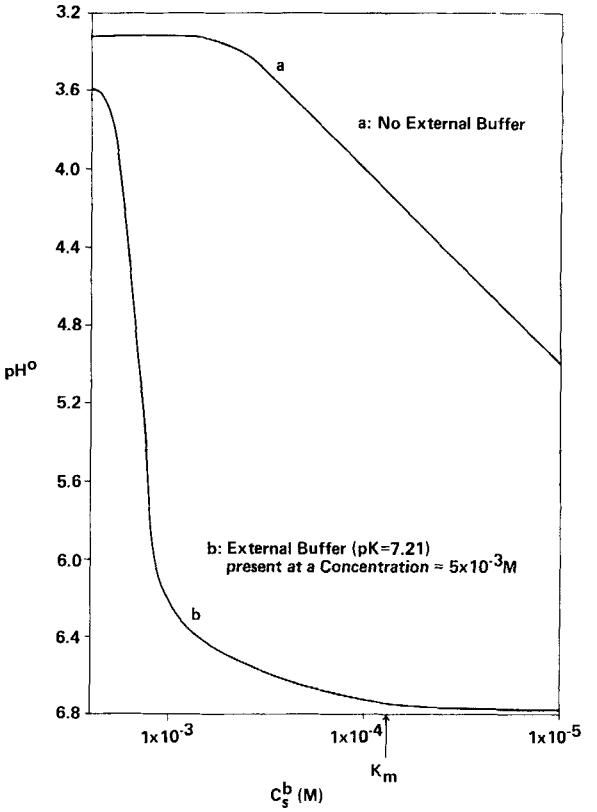

Figure 4. Computed response behavior of an enzyme-pH electrode with design parameters as in Figure 3, $pH^b = 6.72$.

base case are obtained by simply setting $\gamma_A = 0$, $\gamma_B = 1$, and $K_B \rightarrow \infty$ in the equations derived in the previous section.

Case 2. Enzymic reaction produces a weak acid with $\gamma_A = 1$

Response Behavior of Weak Acid Electrode with No Added Buffer. When the acid generated dissociates only partly and when there is no externally added buffer, the two conservation equations, Eqs. 55 and 61, can still be used to describe the electrode performance, but the apparent diffusion coefficient, D_{app}, of protons in Eq. 61 changes. The new expression is obtained by setting $\gamma_A = 1$, $\gamma_B = 0$, and $C^b_{TW} = 0$ in Eq. 47, and is:

$$D_{app} = D\left[1 + \frac{2C_{H^+} - C^b_{H^+}}{K_A}\right] \quad (64)$$

In curve *a* of Figure 5, the electrode response obtained by numerically solving the pair of Eqs. 55 and 61, with D_{app} given by Eq. 64, is plotted for the parameter values in the figure caption. Figure 6a shows the intramembrane substrate and pH profiles leading to the computed electrode response. As shown by curve *a* of Figures 5 and 6a, the electrode exhibits a linear response over the range of C^b_S values for which the fractional substrate concentration drop across the membrane is close to unity (i.e., up to $\sim 2 \times 10^{-3}$ M). For higher C^b_S values, the response starts to become nonlinear and eventually saturation of the electrode occurs for $C^b_S > 5 \times 10^{-3}$ M. It seems surprising, at

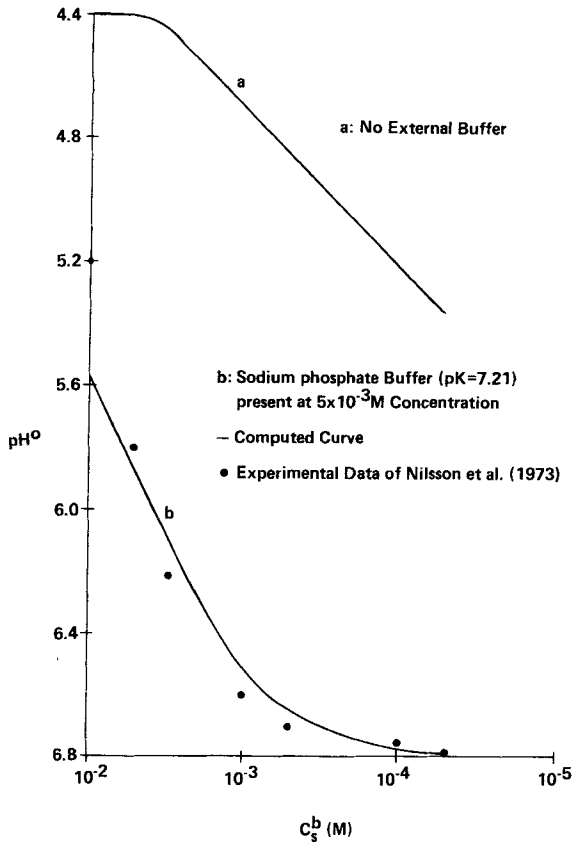

Figure 5. Response behavior of penicillinase-pH electrode. Parameter values:

$\phi = 18.8$ $K_M = 7.7 \times 10^{-5}$ M
$K_1 = 10^{-4.85}$ M $K_A = 10^{-6.4}$ M
$K_2 = 10^{-8.6}$ M $pH^b = 6.72$

first, that the computed response is linear when $f \rightarrow 1$, because Eq. 65 (which can be deduced from Eq. 50 for the present case) seems to indicate nonlinear response in this limit:

$$C_S^b \simeq (C_{H^+}^O - C_{H^+}^b)\left(1 + \frac{C_{H^+}^O}{K_A}\right) \tag{65}$$

However, when $C_{H^+}^O \gg C_{H^+}^b$ and $C_{H^+}^O \gg K_A$, Eq. 65 becomes:

$$pH^o \simeq (-\tfrac{1}{2} \log C_S^b + \tfrac{1}{2} pK_A). \tag{66}$$

The above two inequalities necessary for Eq. 66 to be valid are always satisfied because:

1. the degree of product-acid dissociation is of concern only when the pK_A is approximately equal to pH^b (If $pK_A \ll pH^b$, the dissociation of the acid will essentially be complete and one recovers the strong acid case. On the other hand, if $pK_A \gg pH^b$ the product acid does not dissociate at all, and hence there will be no H^+ ion generation.)

2. $C_{H^+}^O$ is always greater than $C_{H^+}^b$ in the absence of added buffer, see Figure 6a. Therefore, one expects the electrode response to be a linear function of log C_S^b with a slope of -0.5 for the range of C_S^b values in which $f \rightarrow 1$, and this is exactly what is observed in Figure 5a.

It is interesting to note in this context that under identical conditions for a strong acid product, pH^O varies linearly with log

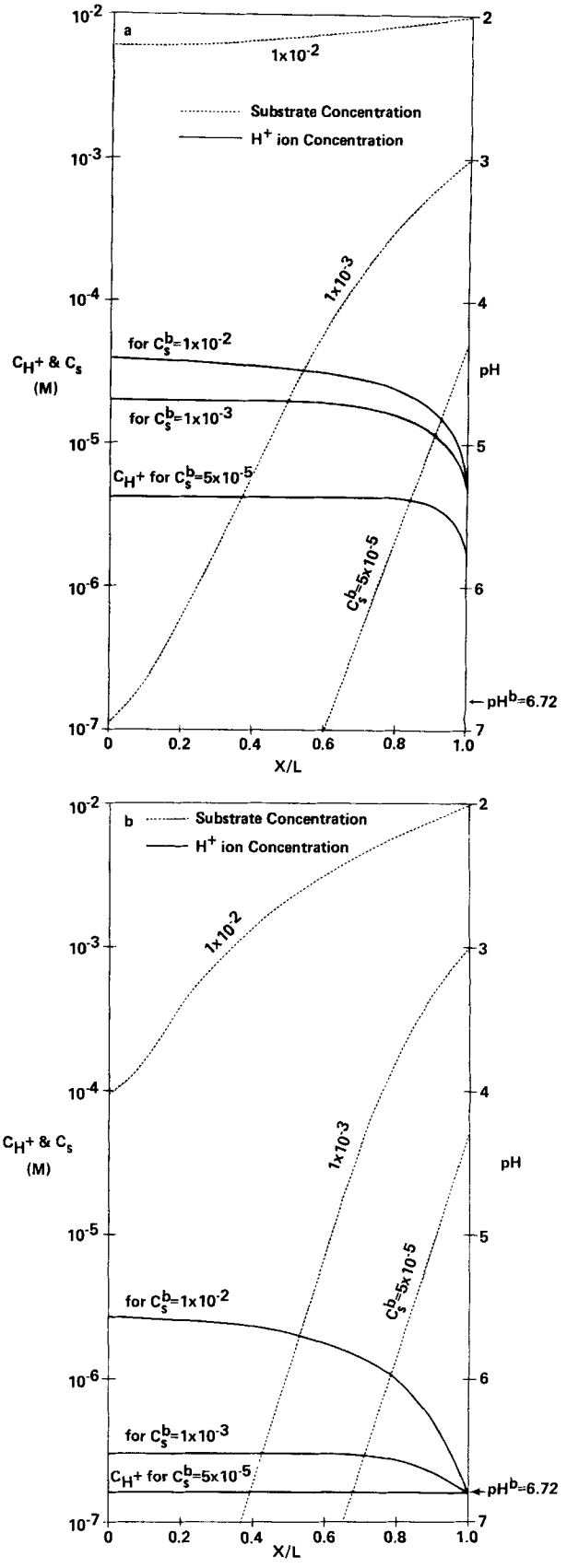

Figure 6. Computed intramembrane substrate and pH distribution profiles for penicillinase-pH electrode having response plotted in Figure 5.

C_S^b at very low C_S^b values, but the slope of this line was -1, instead of -0.5, (see curve *a*, Figure 4), implying a more intense signal from the enzyme-pH electrode. Of course, in this latter case the C_S^b values up to which linearity prevails are much lower compared to the present case, and also saturation of the electrode occurs at much smaller values of $C_S^b (C_S^b \simeq 5 \times 10^{-3}$ M).

Effect of Buffers on Weak-Acid Electrodes. The effect of added buffers in this case is more pronounced than when the product acid is strong, as indicated by the following expression for D_{app}

$$D_{app} = D\left\{\left[1 + \frac{C_{TW}^b K_W}{(K_W + C_{H^+})^2}\right]\frac{(K_A + C_{H^+})}{K_A} + \left(\frac{C_{H^+} - C_{H^+}^b}{K_A}\right)\left[1 + \frac{C_{TW}^b K_W}{(K_W + C_{H^+}^b)(K_W + C_{H^+})}\right]\right\} \quad (67)$$

which is obtained by setting $\gamma_A = 1$ and $\gamma_B = 0$ in Eq. 47. The response behavior of the electrode can be computed in this case by simultaneously solving Eqs. 55 and 61 after substituting Eq. 67 for D_{app}. Once again, Figure 6b reveals the dramatic alterations in the intramembrane pH and substrate concentration distributions resulting from the addition of an extremely small amount ($=5 \times 10^{-3}$ M) of a buffer (with a pK of 7.2) to the bulk solution of the electrode of Figure 6a. Indeed, the added buffer raises the activity level of the membrane to a high value, allowing it to function under substrate diffusion-controlled conditions (i.e., $f \rightarrow 1$) even at a value of 10^{-2} M for C_S^b (compare Figures 6a and 6b). Once again the fact that f was made by the presence of the buffer to approach unity over a large concentration range allows one to predict the electrode response by the following simple algebraic equation:

$$C_S^b = (C_{H^+}^O - C_{H^+}^b)\left[1 + \frac{C_{TW}^b K_W}{(K_W + C_{H^+}^b)(K_W + C_{H^+}^O)}\right]\frac{(K_A + C_{H^+}^O)}{K_A} \quad (68)$$

This equation is obtained by setting $\gamma_A = 1, \gamma_B = 0$, and $C_S^O \ll C_S^b$ in Eq. 50. Curve *b* of Figure 5 displays the response behavior predicted by Eq. 68 for the same electrode whose response in the absence of added buffer was shown in curve *a*.

The design as well as the kinetic parameters used in computing curve *b* in Figure 5 and the profiles in Figure 6b are those corresponding to the penicillinase-pH electrode developed by Nilsson et al. (1973) for monitoring penicillin-G. From the thickness of the membrane used in their experiments, the enzyme loading of their membrane, and the kinetic parameters of penicillinase (Waley, 1975) we computed that the experimental electrode of Nilsson et al. had a Thiele modulus of 18.8. In their experiments, Nilsson et al. maintained the bulk solution at the optimal pH of the enzyme and investigated the electrode response in the presence of 5×10^{-3} M sodium phosphate buffer for bulk substrate concentrations ranging from 5×10^{-5} to 1×10^{-2} M. As was already noticed from Figure 6b, under these conditions $f \rightarrow 1$ for the entire range of substrate concentrations investigated by these authors. Accordingly, Eq. 68 describes the response of their electrode. The experimental data of Nilsson et al. are shown as filled circles in Figure 5. It is indeed gratifying to note that Eq. 68 correctly predicts the experimental response behavior of this electrode.

Further, when (1) $K_A \simeq C_{H^+}^b$, (2) $K_W \sim C_{H^+}^b$, and (3) $C_{H^+}^O \gg C_{H^+}^b$, Eq. 68 takes the following form:

$$pH^O \simeq -\log C_S^b + \log\left(\frac{C_{TW}^b}{2K_A}\right) \quad (69)$$

Thus, under these conditions the electrode response is linear with respect to log C_S^b. As already mentioned, the degree of dissociation of the product acid affects the electrode response only if $K_A \simeq C_{H^+}^b$, and the effectiveness of the added buffer is maximized only if its pK $\simeq$ pH^b. Thus conditions (1) and (2) above are, in general, satisfied. However, $C_{H^+}^O$ is greater than $C_{H^+}^b$ in the presence of added buffers only at relatively large values of C_S^b; at low C_S^b values buffers tend to totally eliminate the intramembrane pH gradients; see Figures 3b and 6b. It is, therefore possible to obtain a linear response from the electrode in the presence of added buffers at high C_S^b values, precisely the range of C_S^b values for which in the absence of buffers saturation of the electrode occurs. At low values of C_S^b, however, the electrode's response becomes nonlinear and is also severely diminished in its intensity by the addition of buffers. However, note from curve *a* in Figure 5 that in the substrate concentration range where the electrode's response is mitigated by the presence of added buffer, one obtains a linear, highly intense response in their absence. In view of these observations, the following strategy for the operation of penicillinase-pH electrodes is proposed. At low values of C_S^b, no externally added buffers should be employed; when, however, C_S^b values are reached where the electrodes tend to prematurely saturate, addition of a small quantity of buffer with a proper pK allows one to achieve a linear response up to the values of C_S^b determined by Brady and Carr's correlation.

Case 3. Enzymic reaction produces a weak acid and a weak base

Nilsson et al. (1973) developed an electrode for monitoring urea in physiological fluids. The hydrolysis reaction results in the formation of two moles of NH_3 and one mole of H_2CO_3 for each mole of urea consumed. H_2CO_3 and NH_3 undergo deprotonation and protonation instantaneously, according to Eqs. 51d and 51e, which have equilibrium constant values of $10^{-6.35}$ and $10^{+9.25}$ M, respectively, at 25°C. It follows that for all pH values less than approximately 9, the hydrolysis of urea leads to a net consumption of H^+ ions. The number of moles of H^+ ions used up per mole of urea consumed is dependent on the actual pH of the medium, and drops from 1.14 to zero in the pH range between 7 and 9, as shown in Figure 7.

Dixon et al. (1980) showed that for urease the dependence of V_{max} upon pH is more complicated than for most other enzymes because urease has two ionization states which can decompose into products.

$$SEH_3 \underset{+H^+}{\overset{K_{SEH_3}}{\rightleftharpoons}} SEH_2^- \underset{+H^+}{\overset{K_{SEH_2}}{\rightleftharpoons}} SEH^- \overset{K_{SEH}}{\rightleftharpoons} SH^- \quad (70)$$

SEH_2^- $\downarrow k_1$ products; SEH^- $\downarrow k_2$ products

Here SEH_i denotes the enzyme-substrate complex (with $i = 0$, 1, 2, 3 representing the different ionization states of the complex). Capital K's denote dissociation constants, and lower case k's denote the rate constants for the formation of products. Using kinetic data obtained at 38°C, Dixon et al. determined the

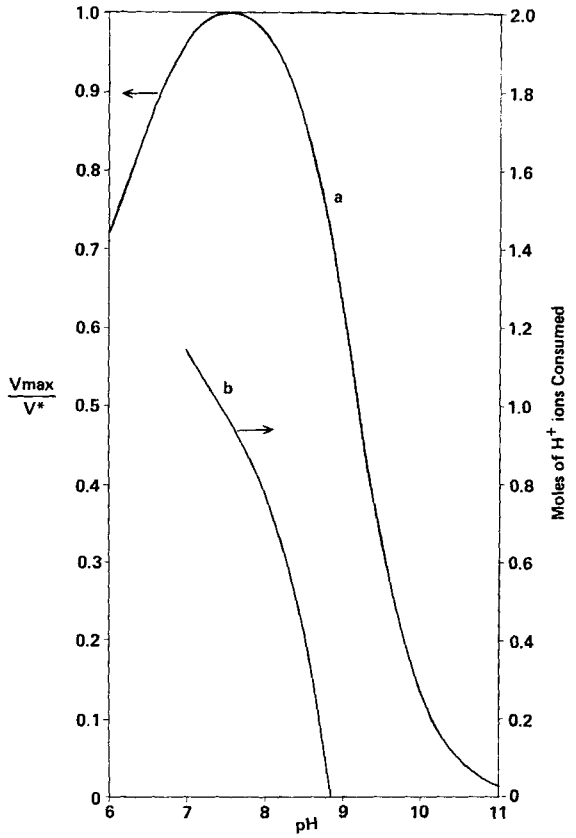

Figure 7. Curve a. Normalized maximum limiting activity V_{max}/V^* of urease vs. pH at 38°C.
Curve generated from Eq. 71: $k_1 = 3{,}600\ s^{-1}$; $k_2 = 6{,}350\ s^{-1}$; $K_{SEH_2} = 10^{-6.25}$ M; $K_{SEH} = 10^{-9}$ M (Dixon et al., 1980)
Curve b. Number of moles of H^+ ions consumed per mole of urea reacting vs. pH.

following values for the constants involved in the above mechanism: $K_{SEH_3} = 10^{-3}$ M, $K_{SEH_2} = 10^{-6.25}$ M, $K_{SEH} = 10^{-9}$ M, $k_1 = 3{,}600\ s^{-1}$, and $k_2 = 6{,}350\ s^{-1}$. These authors also ascertained that for the urease reaction, the Michaelis constant K_M is independent of temperature and exhibits a very weak dependence on pH for pH values greater than 6—the pH range pertinent for use of the electrode in physiological fluids. (They report a value of 2.9×10^{-3} M for K_M in the pH-independent range). From the value of K_{SEH_3}, one can immediately infer that the fraction of the total enzyme in the form of SEH_3 will be negligible for pH values greater than 6, in which case the above mechanism leads to the following expression for V_{max} (Stevens, 1986):

$$V_{max} = \frac{k_1 e_o}{\left(1 + \frac{K_{SEH_2}}{C_{H^+}} + \frac{K_{SEH_2}K_{SEH}}{C_{H^+}^2}\right)} + \frac{k_2 e_o}{\left(1 + \frac{C_{H^+}}{K_{SEH_2}} + \frac{K_{SEH}}{C_{H^+}}\right)} \quad (71)$$

The variation of V_{max} with pH at 38°C is shown in Figure 7. (Since the pH of physiological fluids ~7.4, one can infer from the figure that when urease-pH electrode is immersed in body fluids, the intramembrane pH rise caused by the consumption of protons in the hydrolysis reaction may, unlike with many other enzymes, not necessarily lead to appreciable activity loss—particularly if the pH rise in the membrane is within 1.5 units.) The two coupled equations, Eqs. 24 and 40, in which D_{app} is given by Eq. 47, determine the response of the urease-pH electrode in the presence of added buffers. For urease, Eq. 71 replaces Eq. 53 in the expression of $R(C_{H^+}, C_S)$. We compared the predictions of this model with the experimental data of Nilsson et al. (1973).

They prepared two types of urease-pH electrodes. In the first, urease was immobilized in a polyacrylamide gel membrane that was cast on a pH electrode's bulb, and in the second type a porous cellophane dialysis membrane impregnated with the enzyme solution was wrapped around a pH electrode. The type I electrode was tested for its performance in physiological fluids, while type II was used at room temperature to determine the electrode's behavior as a function of the buffer concentration of the bulk solution. The model predictions are compared with the data on both types of electrodes and the results are shown in Figures 8 and 9, respectively. From the limited experimental information provided by Nilsson et al. it was not possible to estimate the value of $\phi\,[=(k_1 e_o \ell^2/DK_M)^{1/2}]$ for either of the two types of electrodes. However, for the type I electrode, the thickness of the experimental membrane (~400 μm) and the high enzyme loadings employed by the authors appeared to indicate a very large value of ϕ. When ϕ is large, one expects f to approach unity as long as there is no appreciable loss in the enzymic activity of the membrane due to reaction-generated pH gradients. In this case, the response of the electrode can be predicted from the simple Eq. 50 as explained in the earlier section on substrate concentration expressed in terms of proton concentration. Indeed, the sodium acetate buffer present in the physiological salt solution used in the experiments alleviates large intramembrane pH gradients by facilitating proton transport, and hence f does approach unity for the type I electrode. This is indicated by the excellent agreement between the response behavior computed

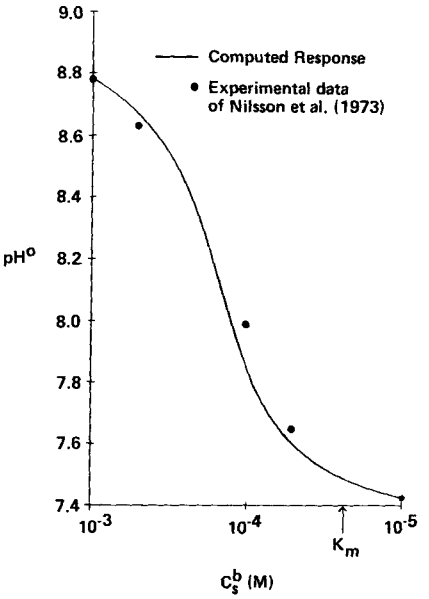

Figure 8. Steady state response of urease-pH electrode (polyacrylamide entrapped) in a physiological salt solution containing sodium acetate buffer.
37°C; $pH^b = 7.4$; buffer pK = 4.76; concentration = 5.8×10^{-2} M. Response computed using Eq. 50 with $C_S^o = 0$ and constant values:
$C_{TW}^b = 5.8 \times 10^{-2}$ M $\quad K_B = 10^{+9.25}$ M
$K_W = 10^{-4.76}$ M $\quad \gamma_A = 1$
$K_A = 10^{-6.35}$ M $\quad \gamma_B = 2$

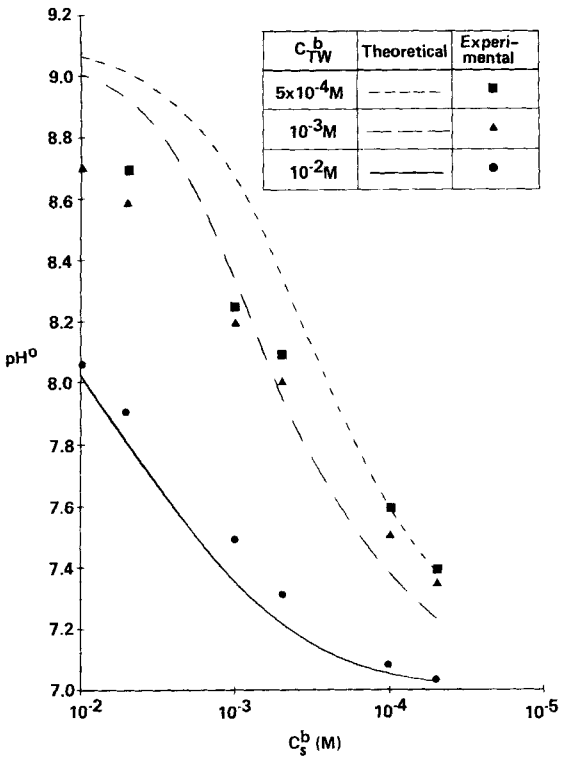

Figure 9. Steady state response of urease-pH electrode for three concentrations of Tris buffer in bulk solution.

25°C; buffer pK = 8.15; pH^b = 7.0 in all three cases
Parameter values:
$K_M = 2.9 \times 10^{-3}$ M k_1 (25°C) = 2,200 s^{-1}
$K_{S\epsilon H_2} = 10^{-6.25}$ M k_2 (25°C) = 4,000 s^{-1} (Dixon et al., 1980)
$K_{S\epsilon H} = 10^{-9.15}$ M $\phi = (k_1 e_o \ell^2 / DK_M)^{1/2} = 2.1$

using Eq. 50 and the experimental data of Nilsson et al., Figure 8.

For the cellophane-trapped membrane, ϕ was varied to match the computed response with experiment for a single C^b_S (10^{-2} M) at $C^b_{TW} = 10^{-2}$ M. The same value of ϕ was used further to predict the response for all other C^b_S values at $C^b_{TW} = 1 \times 10^{-2}$ M, as well as the response behavior corresponding to $C^b_{TW} = 10^{-3}$ M and 5×10^{-4} M. This value of ϕ is 2.1. As can be noted from Figure 9, the computed response does display all the experimentally observed trends and is in fair quantitative agreement with the data. It should be pointed out that the computations for this case were based on the pair of differential equations, Eqs. 24 and 40, not on Eq. 50, since f in this case does not approach unity.

Conclusions

In view of the availability of highly stable and extremely accurate pH sensors, the use of conventional pH electrodes in conjunction with immobilized enzymic membranes seems to provide a very versatile and accurate enzyme electrode for monitoring a large number of biochemicals that lead to H^+ ion formation or consumption during the enzymic reaction. For these electrodes the physiochemical phenomena occurring in the immobilized enzymic membrane are more complex than those of other product-sensitive enzyme electrodes because:

1. The activity of the enzyme is sensitive to its microenvironmental pH
2. The degree of protonation/deprotonation of the product acids and/or bases is dependent upon the pH
3. Externally added buffers can augment the flux of protons through the membrane

It is now established (Brady and Carr, 1980; Gough and Leypoldt, 1981) that one can obtain unsaturated response from product-sensitive enzyme electrodes up to substrate concentrations orders of magnitude greater than the Michaelis constant, K_M, of the enzymic reaction by designing the electrode such that it operates in a diffusion-controlled mode (i.e., at high Thiele modulus values) for the substrate. In the case of enzyme-pH electrodes, large intramembrane pH gradients developing at these high ϕ values drastically reduce the membrane's enzymic activity, forcing the electrode to function in a reaction-controlled mode. The efficient design of enzyme-pH electrodes therefore requires the fulfillment of a rather peculiar and stringent criterion, according to which the electrode should perform under substrate diffusion-limited conditions while the transport resistance for the product (namely, H^+ ions) should be neither large nor negligible, but properly controlled.

It is shown here, by employing a mathematical model that incorporates all the above-mentioned phenomena, that by designing enzyme electrodes with high enough Thiele modulus values and by appropriately controlling the amount of added buffer, it is possible to obtain unsaturated (and even linear) response behavior with enzyme-pH electrodes for substrate concentrations much higher than K_M. Further, when the electrode is designed to meet the above criterion, its steady state response does not depend on the actual kinetics of the enzymic reaction and can be described by means of a simple algebraic equation.

The developed model can account for the simultaneous formation of a weak acid and a weak base during the enzymic reaction. A urease-pH electrode useful for monitoring urea concentration in physiological fluids is used as an example where the enzymic reaction leads to the formation of both a weak acid (H_2CO_3) and a weak base (NH_3). The performance of enzyme-pH electrodes that involve the formation of only a weak acid or a weak base can be obtained as special cases of this more general treatment.

The predictions of this model are found to be in excellent agreement with the experimental data on the penicillinase-pH electrode, and the urease-pH electrode developed by Nilsson et al. (1973) for monitoring penicillin-G and urea, respectively.

Acknowledgment

This research was sponsored by Grant No. CPE-8404298 from the Chemical and Biochemical Processes Program of the National Science Foundation, and a faculty research award from the University of Toledo to S. Varanasi.

Notation

A^-, AH = conjugate base and acid components of product weak acid
B^+ = conjugate acid of product base BOH
BOH = basic product of the enzyme-catalyzed reaction
$\overline{C}$ = dimensionless hydrogen ion concentration = C_{H^+}/K_1
C_i = concentration of species i
$\overline{C_S}$ = dimensionless substrate concentration = C_S/K_M
C_{TA} = total concentration of product weak acid = $C_{AH} + C_A$

C_{TB} = total concentration of product weak base = $C_{BOH} + C_{B^-}$
C_{TW} = total concentration of externally added buffer weak = $C_{W^-} + C_{WH}$
D_{app} = concentration-dependent apparent diffusion coefficient of H^+ ions
D = diffusion coefficient
e_o = total enzyme concentration (includes all forms of the enzyme and enzyme-substrate complexes)
f = fractional change in substrate concentration between two faces of membrane = $(C_S^b - C_S^o)/C_S^b$
F = fraction of the enzyme in catalytically active form = $1/[1 + (C_{H^+}/K_1) + (K_2/C_{H^+})]$
F^o = F value corresponding to optimal pH of enzyme
k = rate constant for decomposition of enzyme-substrate complex
K = dissociation/association constant of acid/base
$\bar{K}$ = ratio of dissociation constant of externally added weak acid to protonation equilibrium constant of enzyme = K_W/K_1
k_f, k_b = forward and reverse rate constants of proton association/dissociation reactions for weak acid/base conjugate pairs
k_1, k_2 = rate constants for decomposition of enzyme-substrate complex into products for urea hydrolysis, Eq. 70
K_1, K_2 = equilibrium constants of protonation and deprotonation reactions of enzyme or enzyme substrate complex
K_M = Michaelis constant
$K_{SEH_3}, K_{SEH_2}, K_{SEH}$ = equilibrium dissociation constants of SEH_3, SEH_2^-, and SEH^-, respectively, Eq. 70
ℓ = thickness of membrane (= L in figures)
R = enzymic reaction rate (moles of substrate consumed per unit volume and unit time), Eq. 52
r_i = molar rate of consumption of species i per unit volume
S = substrate of enzyme-catalyzed reaction
$SEH_3, SEH_2^-, SEH^-, SE^=$ = the four possible protonation states of urease-urea complex, Eq. 70
V^* = maximum limiting rate reached if all immobilized enzyme is in its catalytically active form, Eq. 54
V_{max} = maximum limiting rate at a given pH, Eq. 53
W^- = conjugate base of externally added buffer
WH = conjugate acid of externally added buffer
x = distance coordinate; origin is membrane-electrode interface

Greek letters

γ = stoichiometric coefficient, Eq. 1
ΔpH = change in pH from membrane-electrode interface to bulk = $pH^O - pH^b$
χ = ratio of deprotonation to protonation equilibrium constants of enzyme = K_2/K_1
λ = ratio of Michaelis constant to protonation equilibrium constant of enzyme = K_M/K_1
ϕ = Thiele modulus defined to characterize diffusional resistance for transport of substrate = $(V^* \ell^2/DK_M)^{1/2}$
$\phi' = \phi\sqrt{F^o} = (V_{max}\ell^2/DK_M)^{1/2}$
ξ = dimensionless distance coordinate = x/ℓ

Superscripts

b = value of variable in bulk solutions
O = value of variable at membrane-electrode interface

Subscripts

A = acid product of enzyme-catalyzed hydrolysis reaction
B = basic product of enzyme-catalyzed hydrolysis reaction
i = ith species
S = substrate
W = externally added weak acid

Literature cited

Bailey, J. E., and D. F. Ollis, *Biochemical Engineering Fundamentals*, McGraw-Hill, New York, 128 (1977).

Berjonneau, A. M., G. Brown, and D. Thomas, "Realization of Enzyme Electrodes Using Amino Acid Decarboxylase," *Pathol. Biol.*, **22**, 497 (1974).

Blaedel, W. J., T. R. Kissel, and R. C. Bogusalski, "Kinetic Behavior of Enzymes Immobilized in Artificial Membranes," *Anal. Chem.*, **44**, 2031 (1972).

Brady, J. E., and P. W. Carr, "Theoretical Evaluation of the Steady-State Response of Potentiometric Enzyme Electrodes," *Anal. Chem.* **52**, 977 (1980).

Caras, S. D., J. Janata, D. Saupe, and K. Schmitt, "pH-Based Enzyme Potentiometric Sensors. 1: Theory," *Anal. Chem.*, **57**, 1917 (1985a).

Caras, S. D., D. Petelenz, and J. Janata, "pH-Based Enzyme Potentiometric Sensors. 2: Glucose-Sensitive Field Effect Transistor," *Anal. Chem.*, **57**, 1920 (1985b).

Caras, S. D., and J. Janata, "pH-Based Enzyme Potentiometric Sensors. 3: Penicillin-Sensitive Field Effect Transistor," *Anal. Chem.*, **57**, 1924 (1985c).

Carey, G. F., and B. A. Finlayson, "Orthogonal Collocation on Finite Elements," *Chem. Eng. Sci.*, **30**, 58 (1975).

Clark, L. C., "A Family of Polaragraphic Enzyme Electrodes and the Measurement of Alcohol," *Enzyme Engineering*, Wingard, L. B., ed., Wiley-Interscience, New York (1972).

Clark, L. C., and L. Lyons, "Electrode Systems for Continuous Monitoring in Cardiovascular Surgery," *Ann. N.Y. Acad. Sci.*, **102**, 29 (1962).

Cornish-Bowden, A., *Fundamentals of Enzyme Kinetics*, Butterworths, Boston (1979).

Deem, G. S., N. J. Zabusky, and H. Sternlicht, "Association-Dissociation Time-Scale Factor For Proton Transport in Immobilized Protein Membranes," *J. Membr. Sci.*, **3**, (1978).

Dixon, N. E., P. E. Riddles, C. Gazzola, R. L. Blakeley, and B. Zerner, "Jack Bean Urease (EC 3.5.1.5). V: On the Mechanism of Action of Urease on Urea, Formamide, Acetamide, *n*-Methylurea, and Related Compounds," *Can. J. Biochem.*, **58**, 133 (1980).

Engasser, J. M., and C. Horvath, "Buffer-Facilitated Proton Transport: pH Profiles of Bound Enzymes," *Biochim. Biophys. Acta.*, **358**, 178 (1974).

Flanagan, M. T., and N. J. Carroll, "Thin-Film Antimony-Antimony Oxide Enzyme Electrode for Penicillin Determination," *Biotech. Bioeng.*, **28**, 1093 (1986).

Gough, D. A., and J. D. Andrade, "Enzyme Electrodes," *Science*, No. 1980, 380 (1973).

Gough, D. A. and J. K. Leypoldt, "Theoretical Aspects of Enzyme Electrode Design," *Applied Biochemistry and Bioengineering*, **3**, L. B. Wingard, Jr., E. Katchalski-Katzir, and L. Goldstein, eds., Academic Press, New York (1981).

Guilbault, G. G., *Analytical Uses of Immobilized Enzymes*, Dekker, New York (1984).

Guilbault, G. G., and E. Hrabankoua, "An Improved Electrode for Urea in Blood and Urine," *Anal. Chim. Acta.*, **52**, 287 (1970a).

———, "An Electrode for the Determination of L-Amino Acids," *Anal. Chem.*, **42,** 1779 (1970b).
———, "New Enzyme Electrode Probes For D-Amino Acids and Asparagine," *Anal. Chim. Acta.*, **56,** 285 (1971).
Guilbault, G. G., and F. R. Shu, "Enzyme Electrodes Based on the Use of a Carbon Dioxide Sensor. Urea and Tyrosine Electrodes," *Anal. Chem.*, **44,** 2161 (1972).
Llendo, R. A., and G. A. Rechnitz, "Enzyme Electrode for Amygdalin," *Anal. Chem.*, **43,** 1457 (1971).
Nilsson, H., A. C. Akerlund, and K. Mosbach, "Determination of Glucose, Urea and Penicillin Using Enzyme-pH Electrodes," *Biochim. Biophys. Acta.*, **320,** 529 (1973).
Ruckenstein, E., and D. G. Kalthod, "Immobilized Enzymes: Electrokinetic Effects on Reaction Rates in a Porous Medium," *Biotechnol. Bioeng.*, **24,** 253 (1982).
Ruckenstein, E., and S. Varanasi, "Transient Behavior of Facilitated Transport through Liquid Membranes," *J. Membr. Sci.*, **12,** 27 (1982).
———, "Acid-Generating Immobilized Enzymic Reactions in Porous Media—Activity Control Via Augmentation of Proton Diffusion by Weak Acids," *Chem. Eng. Sci.*, **39,** 1185 (1984).
Scheller, F., et al., *Biosensors*, **1,** 135 (1985).
Stevens, R. L., "Designs of Enzyme-pH Electrodes," M.S. Thesis, Dept. Chem. Eng., University of Toledo (1986).
Updike, S. J., and G. P. Hicks, "The Enzyme Electrode," *Nature (London)*, **214,** 986 (1967).
Waley, S. G., "The pH-Dependence and Group Modification of B-Lactamase I," *Biochem. J.*, **149,** 547 (1975).
Williams, D. L., A. R. Doig, and A. Korosi, "Electrochemical Enzymatic Analysis of Blood Glucose and Lactate," *Anal., Chem.*, **42,** 118 (1970).
Wingard, L. B., Jr., E. Kotchalski-Katzir, and L. Goldstein, eds., *Applied Biochemistry and Bioengineering*, **3,** Analytical Applications of Immobilized Enzymes and Cells, Academic Press, New York (1981).
Varanasi, S., S. O. Ogundiran, and E. Ruckenstein, "An Algebraic Equation for Predicting the Steady State Response of Enzyme-pH (Electrodes/Field Effect Transistors)," submitted to *Anal. Chem.*
Zabusky, N. J., and G. S. Deem, "Intrinsic Electric Fields and Proton Diffusion in Immobilized Protein Membranes—Effects of Electrolytes and Buffers," *Biophys. J.*, **25,** 1 (1979).

Manuscript received Apr. 9, 1986, and revision received Oct. 6, 1986.